# Quantifying climatic and socioeconomic drivers of urban malaria in Surat, India: a statistical spatiotemporal modelling study

*Mauricio Santos-Vega, Rachel Lowe, Luc Anselin, Vikas Desai, Keshav G Vaishnav, Ashish Naik, Mercedes Pascual*

## Summary

**Background** Cities are becoming increasingly important habitats for mosquito vectors of disease. The pronounced heterogeneity of urban landscapes challenges our understanding of the effects of climate and socioeconomic factors on mosquito-borne disease dynamics at different spatiotemporal scales. Here, we quantify the impact of climatic and socioeconomic factors on urban malaria risk, using an extensive dataset in both space and time for reported *Plasmodium falciparum* cases in the city of Surat, northwest India.

**Methods** We analysed 10 years of monthly P *falciparum* cases resolved at three nested spatial resolutions (seven zones, 32 units, and 478 worker units) with a Bayesian hierarchical mixed model that incorporates the effects of population density, poverty, relative humidity, and temperature, in addition to random effects (structured and unstructured). To reduce dimensionality and avoid correlation of covariates, socioeconomic variables from survey data were summarised into main axes of variation using principal component analysis. With model selection, we identified the main drivers of spatiotemporal variation in malaria incidence rates at each of the three spatial resolutions. We also compared observations to model-fitted cases by quantifying the percentage of predictions within five discrete levels of malaria risk.

**Findings** The spatial variation of urban malaria cases was stationary over time, whereby locations with high and low yearly cases remained largely consistent across years. Local socioeconomic variation could be summarised with three principal components accounting for approximately 80% of the variance. The model that incorporated local temperature and relative humidity together with two of these principal components, largely representing population density and poverty, best explained monthly malaria patterns in models formulated at the three different spatial scales. As model resolution increased, the effect size of humidity decreased, whereas those of temperature and the principal component associated with population density increased. Model predictions accurately captured aggregated total monthly cases for the city; in space-time, they more closely matched observations at the intermediate scale, with around 57% of units estimated to fall in the observed category on average across years. The mean absolute error was lower at the intermediate level, showing that this is the best aggregation level to predict the space-time dynamics of malaria incidence rates across the city with the selected model.

**Interpretation** This statistical modelling framework provides a basis for development of a climate-driven early warning system for urban malaria for the units of Surat, including spatially explicit prediction of malaria risk several weeks to months in advance. Results indicate environmental and socioeconomic covariates for which further measurement at high resolution should lead to model improvement. Advanced warning combined with local surveillance and knowledge of disease hotspots within the city could inform targeted intervention as part of urban malaria elimination efforts.

**Funding** US National Institutes of Health.



*Lancet Planet Health* 2023; 7: e985–98

**Departamento de Ciencias Biológicas and Grupo de Investigación en Biología Matemática y Computacional BIOMAC, Universidad de los Andes, Bogotá, Colombia** (M Santos-Vega PhD); **Barcelona Supercomputing Center, Barcelona, Spain** (R Lowe PhD); **Catalan Institution for Research and Advanced Studies (ICREA), Barcelona, Spain** (R Lowe); **Centre on Climate Change & Planetary Health and Centre for Mathematical Modelling of Infectious Diseases, London School of Hygiene & Tropical Medicine, London, UK** (R Lowe); **Center for Spatial Data Science** (Prof L Anselin PhD) **and Department of Ecology and Evolution** (Prof M Pascual PhD), **University of Chicago, Chicago, IL, USA; Urban Health and Climate Resilience Center of Excellence (UHCRCE), Surat, India** (V Desai MD); **Vector Borne Diseases Control Department, Surat Municipal Corporation, Surat, India** (K G Vaishnav PhD); **Surat Municipal Corporation, Surat, India** (A Naik MD); **Department of Biology and Department of Environmental Studies, New York University, NY, USA** (Prof M Pascual)

Correspondence to:
Dr Mauricio Santos-Vega, Departamento de Ciencias Biológicas, Universidad de los Andes, Bogotá 111711, Colombia
**om.santos@uniandes.edu.co**

## Introduction

Cities are becoming an increasingly important ecosystem worldwide, characterised by large spatial heterogeneity.[1] Urban landscapes exhibit rapid and pronounced environmental variation in both time and space, such as flooding events from extreme rainfall and considerable heterogeneity in local temperatures with differences of 2–10°C.[2–4] Urbanisation has also sharpened heterogeneity in population density and socioeconomic conditions, exacerbating inequalities.[5,6] Pronounced socioeconomic inequalities are evident in the unprecedented scale of vast, informal settlements in low-income and middle-income cities.[7,8] Although such heterogeneity is expected to have important consequences for the spatiotemporal population dynamics of vector-borne diseases, the joint effects of climatic and socioeconomic conditions remain poorly quantified for whole cities and across different spatial scales.[9,10]

## Research in context

### Evidence before this study

Urban landscapes are becoming an increasingly important ecosystem around the globe. Low-income and middle-income countries comprise the world's most urbanised regions, with 70% of their populations living in cities. The large and heterogeneous environments of growing cities challenge the understanding and control of infectious disease dynamics, including diseases transmitted by vectors. Because the major mosquitoes transmitting malaria in Africa (*Anopheles gambiae*) rely on natural habitats for their breeding, the disease is considered a predominantly rural problem, with urbanisation expected to decrease its burden in Africa. The term urban malaria often refers to malaria occurring in the peri-urban environment of cities. By contrast, a truly urban malaria mosquito vector, *Anopheles stephensi*, exists in the Indian subcontinent, which relies on the built-in environment for breeding. Thus, malaria spread occurs within cities, which constitute important regional reservoirs of the parasite despite seasonal and low transmission intensity. A literature search of publications in English performed on July 16, 2017, in Mendeley using the search terms "urban malaria" and "India" returned 161 publications, which were mostly reports on diagnostics or brief reports on the disease, and were mostly cross-sectional rather than longitudinal studies addressing the spatiotemporal variation of disease risk for a whole city, the subject of our work. A relevant exception was a modelling study for the city of Ahmedabad, India, although this study did not address multiple seasons at different spatial scales and the statistical modelling did not incorporate climatic conditions jointly with socioeconomic drivers. Another exception was a study of a Geographical Information System for an urban town in Tamil Nadu, India, which assembled, but did not analyse, the surveillance data in real time together with several potential drivers. As such, the Geographical Information System provides a valuable setting for applying the type of analysis presented here. A second search on Scopus using "*Anopheles stephensi*" as the keyword returned 107 publications, including mostly early entomological studies for India but also a few recent such studies on the effect of temperature on demographic and transmission parameters and recent reports of the mosquito in the Horn of Africa (appendix p 6). This geographical expansion makes urban malaria a future possibility for the African continent, where the disease remains so far largely rural and peri-urban.

### Added value of this study

This study relies on an extensive surveillance dataset of *Plasmodium falciparum* cases for Surat, India, to investigate the variation and drivers of malaria risk in a heterogeneous urban environment. A statistical model for the spatiotemporal variation of cases was developed, which includes both climatic and socioeconomic drivers, with the latter summarised into two principal axes of variation. Model structures were compared across three spatial resolutions, ranging from a few zones to a few hundred units. Seasonal hotspots were shown to be largely stationary in time, which allowed the identification of dominant extrinsic drivers. Our results show how the differential effects of population density, temperature, and humidity modulate year-to-year malaria burden at different spatial scales.

### Implications of all the available evidence

The largely stationary patterns of risk across seasons emphasise the existence of hotspots driven by spatial heterogeneity, and facilitate seasonal prediction for ongoing intervention efforts, including vector control, based on malaria surveillance. Our analyses also show how the importance of different drivers varies with spatial resolution, indicating that deeper sampling at a finer scale (ie, units) is likely to improve spatiotemporal modelling of malaria risk and associated prediction, although sampling at the finest scale (ie, worker units) could reduce predictability. The modelling framework, incorporating climatic predictors and major axes of socioeconomic variation, could be applied to other vector-borne diseases and other cities for which surveillance records are available.

Urbanisation can influence mosquito vectors' ecological and physiological parameters, altering the spread and emergence of mosquito-borne diseases. It can also improve infrastructure and environmental health, leading to better health-care provision.[11] Studies of urban malaria have largely focused on Africa, where the disease remains a predominantly rural problem because the vectors are adapted to breed in rural environments.[12,13] A common view is that urbanisation reduces malaria transmission in African cities due to fewer suitable breeding sites for the vectors,[14] improved access to health-care services, and an increased ratio of humans to mosquitoes.[13] Nevertheless, transmission continues to persist in cities, in some cases at even higher levels than in surrounding rural areas, with low socioeconomic status as a major risk factor typically concentrated in peri-urban locations.[12,14] Continuing adaptation of predominantly rural vectors to the urban environment is an increasingly concerning trend.[11,13]

In contrast to Africa, the Indian subcontinent harbours a truly urban mosquito vector, *Anopheles stephensi*, which can transmit both malaria parasites *Plasmodium falciparum* and *Plasmodium vivax*. The mosquito breeds in various artificial containers within homes and construction sites.[15,16] Given the rapid urbanisation of this region, there is growing interest in the spatiotemporal structure of urban malaria and how it reflects the socioeconomic and environmental heterogeneities of large cities.[17,18] A previous study addressed malaria risk in the city of Ahmedabad in northwest India.[17] The statistical models considered climate factors averaged across the whole city as well as

other drivers but so far only at the mesoscale of districts. Thus, the combined role of local population density, humidity, and high temperatures remains largely undescribed for whole cities and across spatial resolutions.[17,19] Reports of *A stephensi* in Ethiopia,[20,21] Sudan,[22] and Djibouti[23] raise concerns on the future expansion of urban malaria beyond its established current geographical distribution in southern and western Asia.[24,25]

Climate variability and climate change are expected to impact urban areas in particular ways, acting as major determinants of global health.[26] Some researchers have argued that at coarser spatial resolutions (eg, >10 km), the effect of climate in urban areas could be negligible.[27] Others have argued that even at coarse, aggregate scales, the effects of climate change should be evident, not only in cities, but also in large, peri-urban areas.[28] The sensitivity of mosquito vectors to environmental variation at fine spatial scales has been studied,[29–31] with expected complex interactions with local features, such as housing density and material, vegetation cover, and distance to water.[29,32] Because climate variables at coarse resolutions represent averages over large areas, land types, and populations, they tend to hide extremes and can lead to spurious correlations with disease risk.[33,34]

The elimination of urban malaria in India remains a challenge. India's urban population increased from 240 million in 1900 to 1·4 billion in 2020 during the 20th century, extending the problem of malaria to cities. Migrants from rural regions usually settling in slums brought malaria parasites and seeded transmission via *A stephensi* in urban areas and *Anopheles culicifacies* in peri-urban areas.[35] Urban malaria cases account for 6–28% of annual disease incidence, thus necessitating targeted attention. In most urban settings, malaria transmission is related to water stored within homes and to construction sites where the breeding of the vector occurs.[24,36] The disease as a specific problem of cities was first recognised in 1969. An in-depth review committee strongly recommended effective anti-larval measures in urban areas, considered responsible for exporting infection to rural areas in many states.[37] The Urban Malaria Scheme was launched in 1971 in 131 cities and towns to address the urban malaria problem.[36] Control efforts are largely based on recurrent anti-larval measures at breeding sites and malaria treatment through passive case detection.[37]

An extensive surveillance programme in the coastal city of Surat in the northwestern state of Gujarat, India, provides an opportunity to analyse the spatiotemporal variability of the disease across three different spatial resolutions. Here, we use a statistical space-time modelling approach to investigate the spatial distribution of urban malaria risk and the effects of both climatic and socioeconomic drivers within the city. We focus on cases by *P falciparum* because these have been the main concern of control efforts, even though incidence attributed to the less virulent *P vivax* is typically higher. Also, *P falciparum* lacks the relapse characteristic of *P vivax*, and as such, should more directly reflect environmental drivers of vector transmission. For climate, the temperature is well known to affect demographic parameters of the vector and the developmental time of the parasite within the vector.[16] Moreover, relative humidity has recently been shown to influence the interannual variability of the disease at the whole-city level for both Surat and Ahmedabad.[38] Humidity rather than precipitation preceding the epidemic season best explains and predicts the temporal, year-to-year variation in epidemic size.[38] Therefore, we interrogate the spatiotemporal data on more local effects of both temperature and relative humidity, in a socioeconomic context. We are interested in the plausibility of reducing the complexity of the socioeconomic space by considering a low number of dimensions that nevertheless accounts for a substantial fraction of the variance. That is, we seek a parsimonious model of the spatiotemporal variation of the disease for the whole city. We discuss how this approach complements more local and detailed epidemiological studies, how our approach could be coupled with existing efforts to use Geographical Information Systems for urban malaria surveillance, and the implications of our findings for malaria control and elimination efforts in the Indian subcontinent.

## Methods

### Study site and data collection

The city of Surat presents ideal characteristics for our study, given the pronounced environmental and socioeconomic disparities and a well established vector-borne disease surveillance programme. The city is located on the banks of the Tapi River in Gujarat, northwestern India (figure 1). It is one of the fastest-growing Indian cities due to immigration from various parts of Gujarat and other Indian states, with a ten-fold increase in population in the past four decades.[39] The climate is semi-arid, with temperatures ranging from 37°C to 44°C in the summer, minimum values of about 22°C in winter, and averages of 28°C during the monsoon season. Rainfall ranges from 950 mm to 1200 mm per year (appendix p 2), and 90% of rainfall falls during the monsoon season, from June to September.[40]

See Online for appendix

Malaria transmission in Gujarat, including the city of Surat, is considered low and epidemic, with highly seasonal transmission and yearly epidemics of peak incidence between September and November.[41] Surat has an average of 1978 total cases per year (0·17 cases per 1000 population) for *P falciparum* (and 6114 cases per year, or 0·36 cases per 1000 population, for *P vivax*; appendix p 3). Control efforts have reduced the burden of malaria since the epidemic emerged in the 1990s for both parasites in the city. We focus here on *P falciparum* because it remains the main target of control efforts.

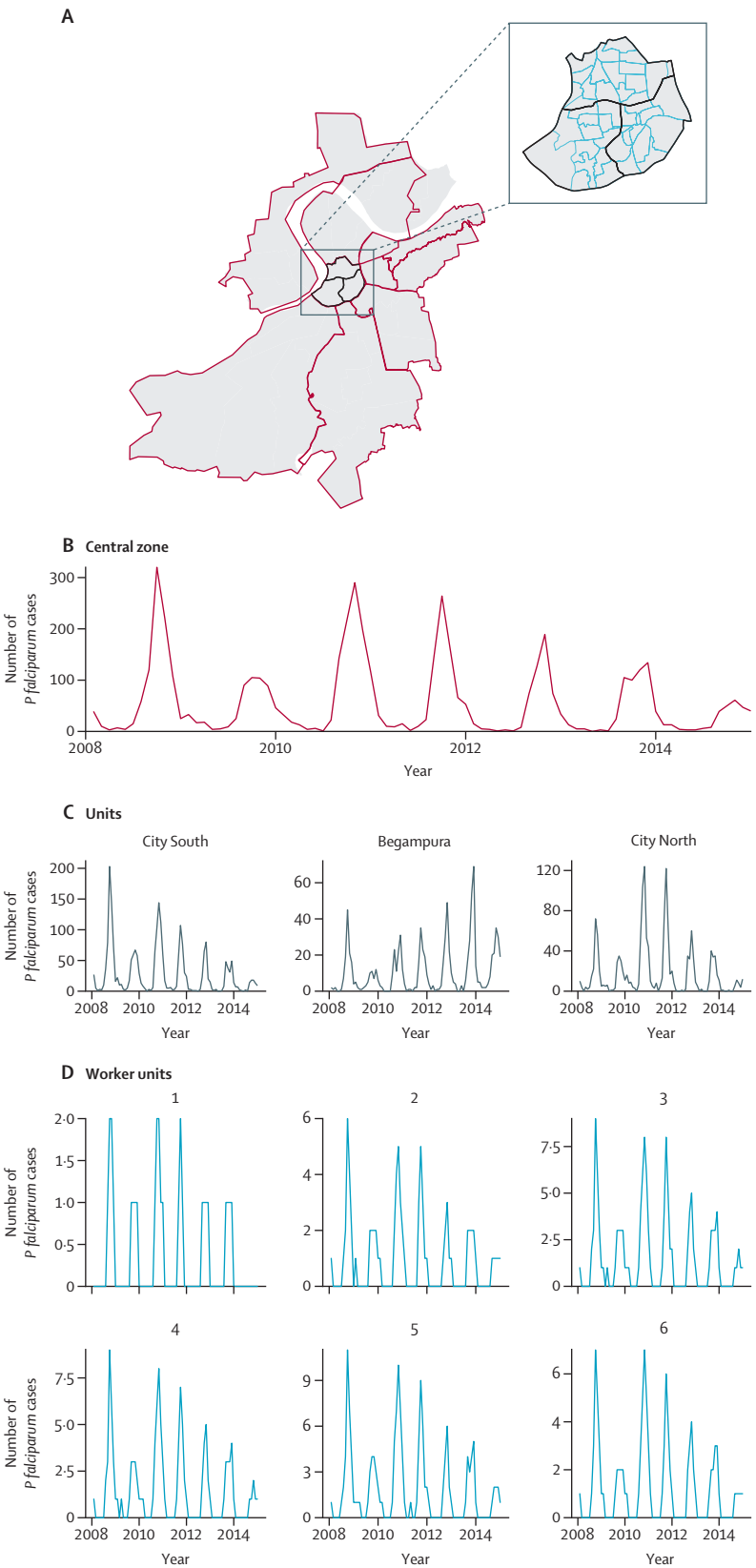


Dedicated control efforts (indoor residual spraying, breeding site detection, or insecticide-treated bednets to prevent transmission) by the Surat Municipal Corporation have kept malaria incidence low but have not eliminated the disease. Malaria still exhibits interannual variability with seasonal outbreaks of varying sizes (appendix p 3).

We obtained monthly malaria cases from 2008 to 2014 from the Surat Municipal Corporation disaggregated at three different levels of spatial resolution corresponding to seven zones, comprising 32 units, which are further divided into 478 worker units. A worker unit corresponds to an area inhabited by approximately 10 000 population, assigned to a malaria control personnel for epidemiological surveillance (both active and passive).

We collated multi-sourced spatiotemporal climatic and socioeconomic datasets. We reconciled the socioeconomic and demographic data to the 1-km grid of the climate data, to generate three databases of malaria cases and associated covariates at the different levels of aggregation. Specifically, an ordinary kriging method (appendix p 14) was used to generate an estimated interpolation surface for each covariate at the level of the 478 worker units.

The socioeconomic data are based on both the 2011 census and a household survey at 90 locations and 400 households (appendix p 14).[39] Additional data on population and slum density were obtained from the Surat Municipal Corporation.

Satellite products were used for the climate data. Land surface temperatures were extracted from both the Terra and Aqua satellites of MODIS, and precipitable water values were acquired from MODIS MOD05_L2 Total Precipitable Water for their overlapping period between 2008 and 2015. Relative humidity is typically associated with precipitable water, land surface temperature, and specific humidity, with high precipitable water values in the absence of clouds indicating a very moist atmosphere.[42] Relative humidity reflects the amount of moisture in the atmosphere; when relative humidity is low, it contributes to the drying of environmental moisture (a measure of the amount of water in the air column and vegetation), and conversely when relative humidity is high, the environment absorbs moisture from the atmosphere. We used these products and relationships to estimate surface relative humidity. Specifically, we calculated specific humidity from precipitable water using a previously

***Figure 1:*** **Map of the study zones and time series of *P falciparum* cases in the central zone in 2008–14**
(A) Study area. The seven administrative zones of Surat, India, are depicted in red. For illustration, selected units (of a total of 32) are shown in black within the central zone. The embedded image shows worker units in blue. A time series of *P falciparum* cases is shown for the central zone (B), and the three units (C) and six worker units (D) within the central zone. *P falciparum*=*Plasmodium falciparum*.

published expression (appendix p 16). We calculated air pressure using a linear association with elevation (appendix p 16) and used land surface temperatures from MODIS. Relative humidity was calculated based on specific humidity, air pressure, and air temperature (appendix p 17). Because satellite climate data are often sensitive to measurement errors, we used observations from ten local temporary meteorological stations to check for the consistency of the satellite products (appendix p 16).

### Data analyses

To examine spatial patterns of malaria risk independently from the interannual variation of incidence, we accumulated reported cases for a given year. We normalised this sum by the total yearly cases for the whole city. We then conducted standard univariate statistical analyses for spatiotemporal systems to evaluate the spatial dependency of malaria cases per 1000 people. Specifically, a univariate Moran Index (Moran's I) was computed through time (appendix p 3).[43,44] Moran's I is used to identify the global degree of spatial association (how much the magnitude of the variable of interest at one location influences its magnitude at a nearby area).[43,44] Given the existence of a significant spatial autocorrelation in the data, we aimed to identify where the hotspots formed by spatially autocorrelated units were located. We used for this purpose a local indicator of spatial association (LISA).[44] This statistic specifically identifies units with a high incidence that are significantly associated with surrounding units also of high incidence. We could therefore identify malaria hotspots and assess whether they were maintained over time.

To reduce the dimensionality of the socioeconomic variables (appendix p 4) and to address the existence of a spatial pattern in these indicators, we used principal component analysis (PCA). This method was applied to find the best low-dimensional representation of the variation in this multivariate dataset, and to determine which variables were associated with each of the major components. In the statistical model described later, we specifically retained components that together account for more than 80% of the variance in socioeconomic space.

### Statistical models

We used a spatiotemporal Bayesian hierarchical model framework to assess the relative contribution of climatic and socioeconomic factors in determining space-time urban malaria case patterns. Generalised linear mixed models (GLMMs) were formulated, including climate covariates (with linear and non-linear terms), PCA terms, and random effects (to account for spatial dependency structures, seasonality, and interannual variability attributed to unobserved factors, such as control efforts, quality of health-care services, and local health interventions).[45–48] The model parameters were estimated in a Bayesian framework in R version 4.0.2 (using integrated Laplace approximations[49,50]). The equations are given and described in the appendix (pp 18–20).

### Scale dependency

Model selection criteria (deviance information criterion and cross-validated mean log score) were applied to identify the best model at a given resolution (starting with the intermediate scale of units). Then, to evaluate the model sensitivity to a change in spatial scale, we also compared the likelihood ratio pseudo-$R^2$ and the mean absolute error (MAE) of the best model selected at the intermediate level of aggregation with those selected at both the more aggregated resolution (seven zones) and the more disaggregated resolution (478 worker units). Although it is interesting to compare the model performance at different scales, we focused on understanding a comparison of the factors that are significant at the different scales; for this, we evaluated changes in the 95% credible interval of the different estimated parameters to determine whether they contained zero.

### Model predictability

To assess the predictive ability of the best model for each spatial resolution, we used the posterior predictive distributions of malaria incidence for each unit and month. To summarise this information, we aggregated annually the observed and posterior predictive mean malaria risk estimates across months and generated predictions for each unit in high and low incidence years. We compared the temporal evolution of the fitted posterior median cases with the observed cases for the entire city of Surat. We first compared the difference in MAE (the average of all absolute errors). We performed comparisons between the baseline model (model with the monthly and yearly random effect) and each new candidate model fitted at each level to identify the proportion of units for which more complex models improved model fit.[51] In addition, we classified the cases into five categories generated by assembling all zero cases in one class and subdividing all remaining non-zero cases into four equally sized intervals (based on quantiles of the distribution of cases). The resulting categories were labelled as no cases, very low, low, high, and very high cases. We then mapped the categories of the spatial predictions and observed cases for 2008 and 2011, and quantified the times that the classes correctly matched. These years were selected to represent a high and low transmission year based on the temporal dynamics (appendix p 3). Finally, we compared the proportion of places where the selected model accurately predicted malaria incidence across scales.

### Role of the funding source

The funders of the study had no role in study design, data collection, data analysis, data interpretation, or writing of the report.

For more on **land surface temperature data from MODIS** see https://earthdata.nasa.gov/eosdis/daacs/laads

For more on **precipitable water data from MODIS** see https://modis.gsfc.nasa.gov/data/dataprod/mod05.php

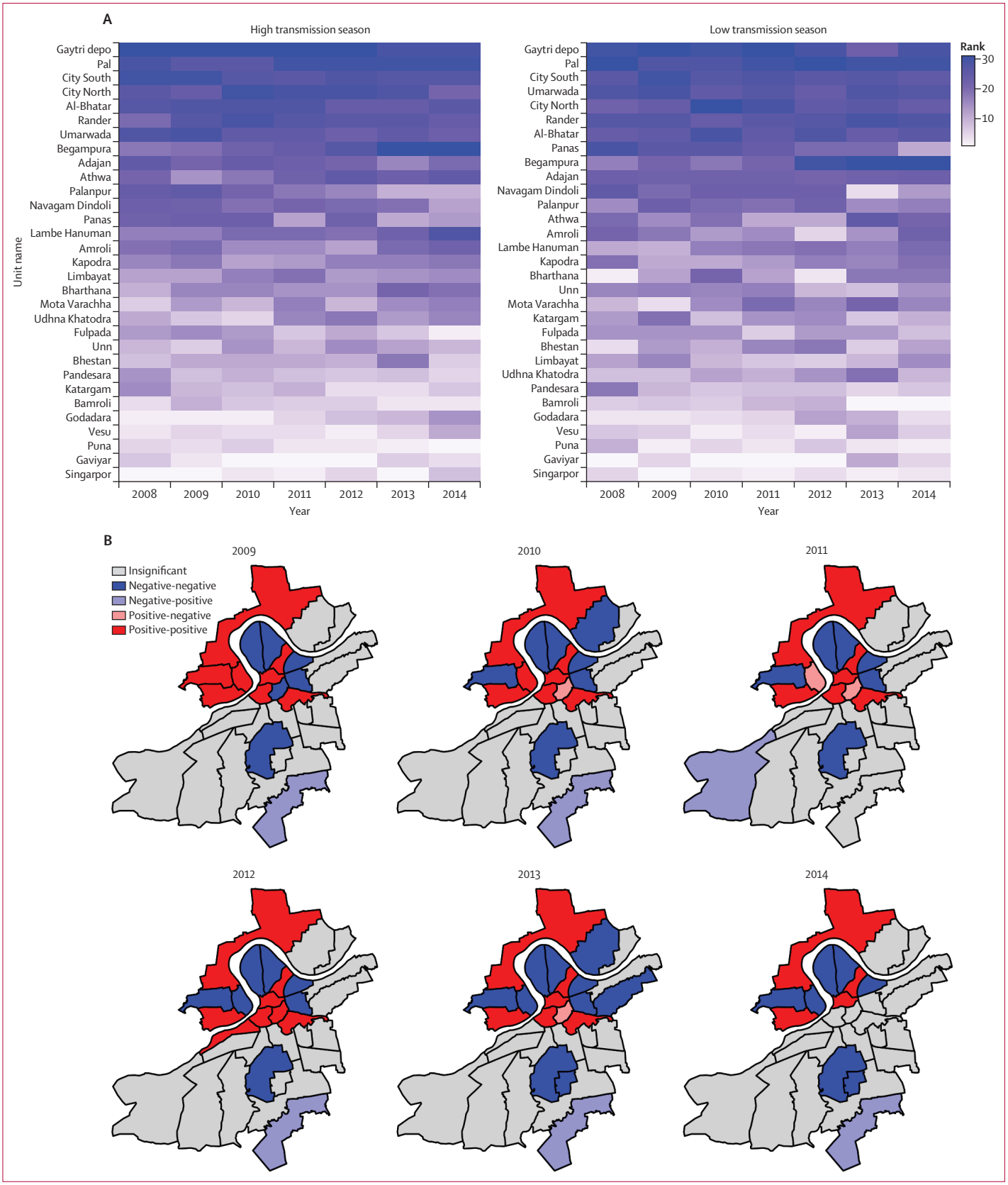
A
High transmission season
Low transmission season
Rank
30
20
10
Unit name
Gaytri depo
Pal
City South
City North
Al-Bhatar
Rander
Umarwada
Begampura
Adajan
Athwa
Palanpur
Navagam Dindoli
Panas
Lambe Hanuman
Amroli
Kapodra
Limbayat
Bharthana
Mota Varachha
Udhna Khatodra
Fulpada
Unn
Bhestan
Pandesara
Katargam
Bamroli
Godadara
Vesu
Puna
Gaviyar
Singarpor
2008
2009
2010
2011
2012
2013
2014
Year
B
2009
2010
2011
2012
2013
2014
Insignificant
Negative-negative
Negative-positive
Positive-negative
Positive-positive

## Results

The pattern that resulted from ranking malaria risk based on incidence was mainly stationary, with locations of high risk and low risk persisting over time (figure 2A), independently from the interannual variation in total malaria cases (figure 1, appendix p 6). This regular spatial pattern suggests the existence of underlying substantial spatial determinants that are largely stationary over the temporal scales of malaria variation considered here. This pattern exhibited spatial autocorrelation as evaluated with Moran's I (appendix p 3); of note, this spatial association was also largely stationary but exhibited seasonal and interannual variation with a slight reduction concomitant with the transient decline in epidemic size during this period (appendix p 3). The LISA test showed that clusters of high versus low malaria risk locations varied across the city (figure 2B). Specifically, units in the central and northern parts of the city showed positive-positive associations with malaria risk or hotspots, whereas some units in the southern periphery showed negative-negative associations or coldspots. This pattern of clusters identified through spatial associations also showed a striking regularity from season to season (figure 2B, appendix p 6).

We used PCA to reduce the dimensionality of the socioeconomic space (appendix p 4). This analysis provides a low-dimensional representation of the variation in this multivariate dataset (figure 3A, B, appendix p 7). The scores in figure 3C show the correlations between specific socioeconomic variables and the different principal components (PCs). PC1 broadly represents the economic level, with contributions including total income and variables related to access to water. PC2 is associated mainly with labour and employment, probably representing the effect of movement and exposure in particular environments within the city. Finally, PC3 exhibits a substantial contribution from population density. These three components accounted for more than 80% of the total variance in the data (figure 3D).

We then addressed the association of malaria risk with the space-time variation in socioeconomic variables, including population density, summarised in the three main components of the PCA and environmental factors incorporated linearly and non-linearly (relative humidity and temperature). The temporal associations between ranked malaria risk and mean temperature and humidity are shown in the appendix (p 8). A statistically significant linear correlation was found only between malaria risk and relative humidity ($p<0·01$). Significant spatial correlations ($p<0·05$) were found between PC1 and PC3 and the mean ranked cases (appendix p 8). These exploratory analyses suggested the covariates that might contribute significantly to the spatiotemporal statistical model for cases across the city.

To identify and select these variables, we considered the results of fitting the different GLMMs of increasing complexity, which incorporate the climatic and socioeconomic factors, as well as random effects accounting for unobserved variation, more formally. Goodness-of-fit metrics for the GLMMs are shown in the table. Models that included or excluded the effect of a given climatic or economic or demographic variable and neighbourhood structure were compared based on DIC and cross-validated mean log score. In addition to the terms of our baseline model (seasonal, annual, and spatial random effects), we found that the model fit was best when the socioeconomic variation summarised in PC1 and PC3 was included (table). For the two climate covariates, we specifically compared model performance for linear and non-linear functions. The DIC scores for the different models with combinations of climate covariates (with lag 0) implemented linearly and non-linearly are shown in the appendix (p 8). For most models, performance was better for the non-linear than for the linear functions. The non-linear association between climate factors and malaria incidence rates is supported by a decreasing non-linear association for temperature and a saturating positive association for humidity (appendix p 9).

The selected model that best accounted for the spatiotemporal variation in malaria incidence included the combined effects of temperature, humidity, PC1 and PC3, and seasonal and spatial random effects. Combined with the random structured and unstructured effects, these factors explained 60% of the variance based on the $R^2$ likelihood ratio test (table). Of the 60% total variance explained, 29% was accounted for by the monthly (seasonality) and yearly unstructured and structured random effects. An additional 10% was accounted for by PC1 and PC3, and another 21% by climate factors (temperature and relative humidity). Specifically, the interannual variability of humidity and temperature affected the temporal variation of malaria cases across the years (appendix p 9).

We showed the posterior mean parameter estimates for the best model at the intermediate level (units; appendix p 10). All parameters differed significantly from zero, with posterior distributions from the two chains well mixed and converged based on the Gelman-Rubin diagnostic.

***Figure 2:*** **Spatiotemporal patterns of malaria annual ranked incidence**
(A) Distribution of cases normalised by population, with colour intensity (from low [white] to high [blue]) corresponding to the ranking of incidence at the level of the unit. (B) Clusters in malaria incidence (cases per 1000 population) for 2008–14 identified using LISA analysis. The resulting LISA cluster maps depict locations with significant local Moran's I statistics, classified by type of spatial association. This analysis explicitly identifies units with a spatial association in malaria incidence. Depending on the indicator's sign (positive or negative), the local associations can be positive-positive (in red), positive-negative, negative-positive, or negative-negative (in dark blue). Positive-positive and negative-negative associations represent spatial clustering, whereas positive-negative and negative-positive correspond to spatial outliers. In this plot, local spatial autocorrelation corresponds to the core of a cluster (the actual cluster includes all the neighbours of a unit and the core). Clusters are significant at $p<0·05$ (based on 9999 permutations). LISA=local indicator of spatial association.

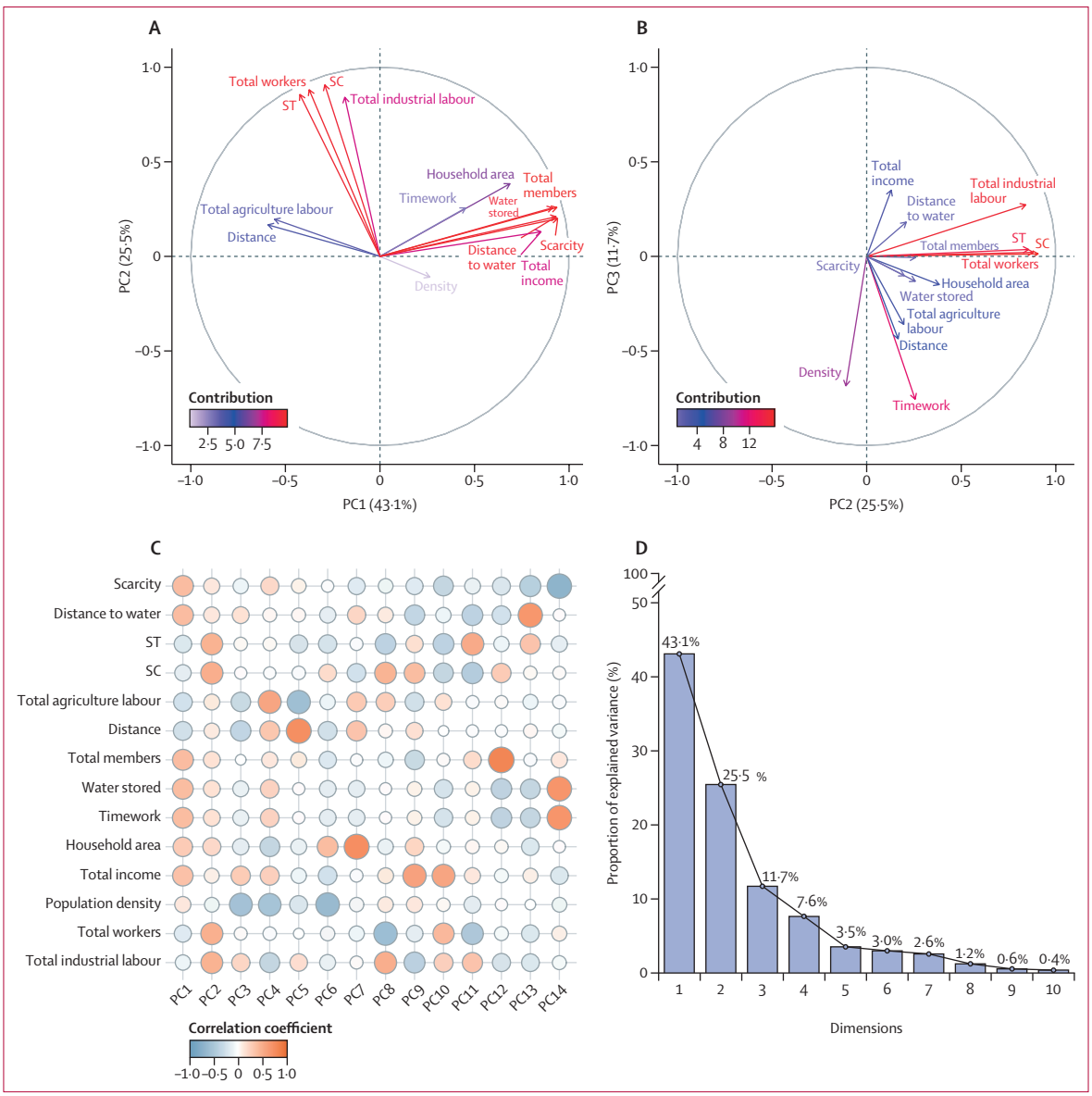


***Figure 3:*** **Principal component analysis of the socioeconomic data**
(A, B) Contribution of the different socioeconomic variables to the three principal axes of variation. Vectors depict the contributions of the socioeconomic variables to two PCs at a time, the first and second in (A) and the second and third in (B). The colours from light blue to red indicate the value of the contributions from low to high. (C) Scores (the transformed variable values in the new space defined by the PCs) or correlation coefficients between the variables (rows) and the PCs (columns). (D) Scree plot showing the contribution of the different components to the total variance in the original data in descending order of importance; the three first components explain 80% of the variance. The association between the PCs and the cases is shown in the appendix (p 8). PC=principal component. SC=Scheduled Caste. ST=Scheduled Tribe.

PC3 exhibited a positive and statistically significant association with malaria incidence. Moreover, the effects of climate factors on malaria incidence rate were non-linear, consistent with our exploratory analyses (appendix p 9). The effect of temperature was negative, consistent with temperatures above a certain threshold decreasing transmission intensity by influencing mosquito and parasite physiological and demographic parameters.[52,53] Relative humidity showed a significant positive effect on malaria risk across the city (appendix p 9)

A comparison of predicted and observed malaria cases is presented in figure 4 (and appendix p 9). In general, predicted and observed cases were consistent over time for the total cases, with a slight tendency to underpredict seasonal peaks (figure 4A). The maps show spatial comparisons for observed and predicted cases at the unit level for representative years, namely 2008 for high incidence (figure 4C, E) and 2011 for low incidence (figure 4D, F). Generally, the predicted patterns reflected the observations for individual units and the mean

| | DIC | Cross-validated mean log score | Likelihood ratio pseudo-$R^2$ |
|---|---|---|---|
| **Baseline: monthly and yearly random effects** | | | |
| Monthly (eg, seasonality) and yearly random effects plus unstructured and structured spatial random effects | 4940 | 3·45 | 0·291 |
| **Baseline plus socioeconomic factors** | | | |
| Baseline plus PC1 | 4927 | 3·33 | 0·354 |
| Baseline plus PC1 and PC2 | 4928 | 3·34 | 0·341 |
| Baseline plus PC1, PC2, and PC3 | 4921 | 3·29 | 0·362 |
| Baseline plus PC2 and PC3 | 4923 | 3·28 | 0·361 |
| Baseline plus PC1 and PC3 | 4913 | 3·06 | 0·396 |
| **Baseline plus socioeconomic factors plus climatic factors** | | | |
| Baseline plus PC1 and PC3 plus spatial temperature (linear) | 4901 | 2·96 | 0·433 |
| Baseline plus PC1 and PC3 plus spatial temperature (non-linear) and humidity (linear) | 4894 | 2·93 | 0·481 |
| Baseline plus PC1 and PC3 plus spatial temperature (non-linear) and spatial humidity (non-linear) | 4899 | 2·95 | 0·600 |

Adequacy results include DIC, cross-validated mean log score (the conditional and marginal coefficient of determination for generalized mixed-effect models1), and $R^2$ based on the log-likelihood from the Bayesian fit comparing the baseline model to each of the other models, for *Plasmodium falciparum* cases in Surat at the intermediate resolution (units). Humidity and temperature denote averages over all the units, whereas spatial humidity and temperature denote their local value for the 32 units. Smaller values indicate better fitting models for the DIC and cross-validated mean log scores. The value of $R^2$ compares observations and predictions (organised into five levels) and provides a measure of the fraction of the total variability explained. DIC=deviance information criterion. PC=principal component.

***Table:*** **Comparison of the goodness of fit for the spatiotemporal statistical models at the intermediate spatial resolution (units)**

seasonality, and for the aggregated total cases over the whole city monthly (figure 4, appendix p 9). The interannual variability of these total cases was well reproduced in these simulations for the whole study period, starting from initial conditions (appendix p 9). In the spatially explicit comparisons, we observed that the models at the intermediate level correctly predicted the observed case quantile in 73% of the units in 2008 and 66% in 2011. In addition, the percentage of units for which the model predicted on average the right case quantile was the highest at the intermediate level (57%), compared with two (29%) of seven units at the aggregated level of zones and 236 (49%) of 478 worker units predicted correctly (appendix p 11). Underprediction of peaks occurred particularly for the city centre in years with low epidemics, such as 2011. By contrast, for years with large epidemics, such as 2008, the model could capture the overall spatial pattern across the southeast and northwest of the city.

To explore whether the significance of the covariates varied as a function of spatial scale, we repeated the model selection process for the other two spatial resolutions of seven zones and 478 worker units. The goodness of fit of the selected models for these two levels is shown in the appendix (p 11). Results were broadly consistent with those at the intermediate scale, in that adding climate and PCs representing socioeconomic or demographic variation improved the fit despite the increased model complexity. In addition, based on the $R^2$ likelihood, we found that, overall, the models at the intermediate scale had a higher goodness-of-fit measure, meaning that they explain a larger proportion of the variance. To further explore the influence of scale, we compared the significance of the fitted coefficients for the respective best models at the three different spatial levels (zones, units, and worker units; figure 5). Although the signs of each coefficient were consistent across scales, and, to some extent, their values were also largely consistent, we were interested in changes in their significance level (parameter estimates were considered statistically significant if their 95% credible interval did not contain zero). The effect of climate covariates contributed to explaining temporal variability in the data. Specifically, when we compared the contribution of the monthly and yearly random effects from the baseline model to those for the best model at each of the levels, the contribution was significantly reduced when we incorporated these covariates (appendix pp 12–13). When we disaggregated the system, the effect of temperature strengthened, whereas that of humidity weakened (figure 5). The effects also intensified for PC1 and PC3 (primarily reflecting the level of income or economically deprived communities and the population density of a site, respectively), both for the value and the significance of the corresponding coefficients from lowest to highest resolution.

To explore the predictive ability of the best models at each of the scales, we evaluated the differences in the MAE. The respective difference in the MAE of a baseline model (in this case, a model with only random effects: seasonal, annual, and spatial) and the best model at each level are shown in the table and appendix (pp 4, 13). This quantity represents a measure of the difference between modelled and observed values, over the 8 years, for each spatial unit. The unit level showed a lower variance in these differences and a higher proportion of locations

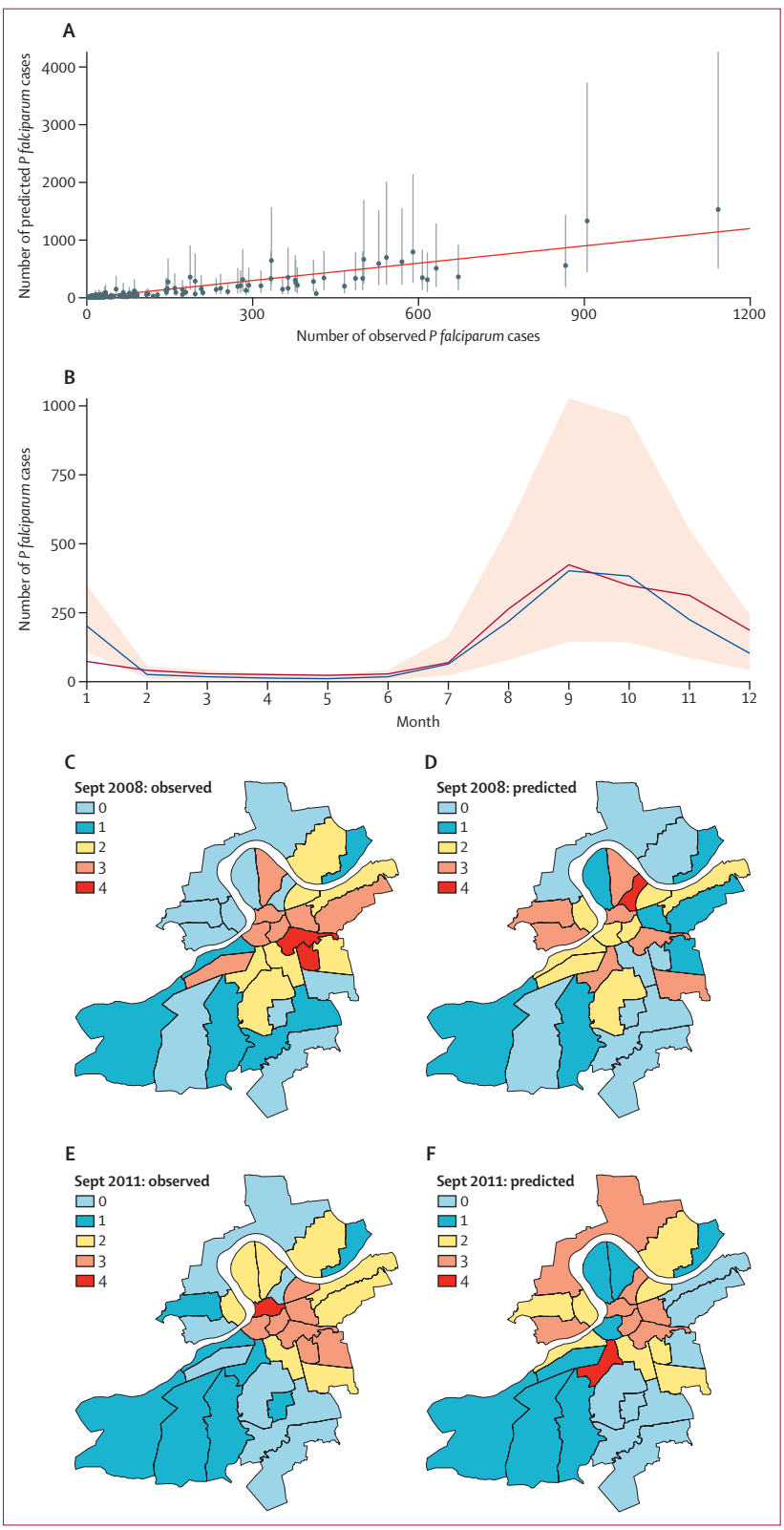


with positive values of the MAE difference (appendix p 13). Thus, adding the climatic and socioeconomic variables improved the model fit for most units. At the finer level of worker units, we saw an interesting pattern with a considerable fraction of locations with positive values of the MAE difference, indicating again that consideration of climatic and socioeconomic conditions improved model performance for most of these units. However, we also saw substantial variance across locations in the MAE difference values, reflecting that there were places with very high improvement and others with very low improvement in predictive power. Finally, at the coarser level of zones, a high fraction of locations showed a negative value for this quantity, reflecting a lower performance of a model incorporating climatic and socioeconomic conditions for most of the regions compared with a model that incorporates only the random effects.

## Discussion

Urban environments show pronounced heterogeneity from rapid and unplanned urbanisation.[18,54,55] Our results underscore the importance of considering this spatial heterogeneity for predicting urban malaria risk in the Indian subcontinent. The spatiotemporal statistical models presented here build upon the results of Santos-Vega and colleagues[17] for a different inland city in northwest India by addressing the combined role of socioeconomic, demographic, and climatic factors in determining malaria risk at different spatial scales. Combining these factors best explains the spatiotemporal variation regardless of spatial scale, from seven coarse zones to more than 400 worker units.

Although both temperature and relative humidity showed significant effects across these spatial scales, the significance of their respective effects increased only for temperature at the finer scales, reflecting a local influence. Thus, the two climate covariates contribute differentially to explain malaria variation: humidity helps capture interannual variability and peak timing of

***Figure 4:*** **Observed versus predicted *P falciparum* cases**
(A) Total *P falciparum* cases. The identity line (in red), a Pearson correlation of predicted versus observed cases, shows a value of 0·65. (B) Seasonal pattern for the observed cases averaged over all years (red) and the median of 1000 model simulations (blue). The 2·5th to 97·5th percentiles of the simulated data are shaded in light red. Comparison of observed (C, D) and predicted (E, F) cases for 2008, a low incidence year (C, E) and 2011, a high incidence year (D, F). The colours in the maps progress from blue to red based on quantiles generated by considering all zero cases in one class and subdividing all remaining non-zero cases into four intervals. The resulting five categories correspond to no cases (0), and a very low (1), low (2), high (3), and very high (4) number of cases. Comparisons of the quantiles in the maps show that 73% of values match for 2008 and 66% match for 2011. *P falciparum*=*Plasmodium falciparum*.

outbreaks; temperature contributes to explaining spatial variation synergistically with socioeconomic covariates. Comparisons across scales indicated that the variation explained by temperature was highest for the highest resolution, whereas that explained by humidity increased for the lower resolution.

The model specifically shows a negative relationship between malaria cases and high temperatures. The negative effect is consistent with the known non-monotonic dependence of malaria's vectorial capacity, and therefore reproductive number, $R_0$, as a function of temperature, which changes from positive to negative as temperature increases beyond the thermal maximum toward the high end of the temperature spectrum.[54–56] As a composite quantity, vectorial capacity incorporates several parameters that also vary as a non-linear function of temperature; these include the incubation period of the parasite within the mosquito, several demographic parameters of the mosquito, such as larval developmental rate and adult survival rate, and parameters related to transmission, such as biting rate and the probability that a bite results in infection (a study in *A stephensi* was done by Villena and colleagues[16]). Consistent with the negative effect in our model, Surat's temperatures fall above the thermal maximum of vectorial capacity and are generally higher than the optima identified for malaria vectors. The negative relationship at high temperatures emphasises the need to better understand thermal dependencies at the high end of the temperature spectrum, the least studied part of the physiological curve.[29,54,57]

The difference between the two climate variables in whether they are most significant at aggregate or local scales could be explained by the strong dependence of relative humidity on winds, which can alter evaporation by changing water vapour in the air. Because winds tend to vary at a regional scale, humidity would also manifest change over large distances.[2] By contrast, temperature can exhibit large variation within a city at the local level, given the pronounced heterogeneity of impervious surfaces, with different radiative, thermal, aerodynamic, and moisture properties.[19] This conclusion should be further examined with a higher number of local humidity measurements on the ground to cross-validate satellite-derived values. Similarly, a higher number of households could be included to describe socioeconomic variation across the city.

Our PCA showed that the presence of three distinct components summarised most of the variability across spatial units in the socioeconomic covariates, with only the first and third proving relevant to the spatiotemporal patterns. The first component largely summarises the effect of economic disparities, which can modulate host exposure to mosquitoes and water availability and management, affecting recruitment of the vector.[15,16,36] Access to water is an important determinant of malaria risk given that water is supplied irregularly in Indian cities, leading to water storage within households,

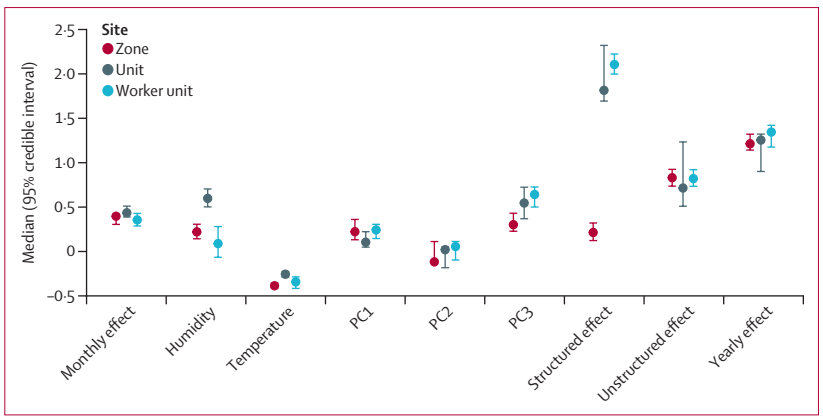


***Figure 5:*** **Model coefficients and their effect size at different spatial scales**
Comparison of parameter estimates for the best respective models at the three levels of aggregation (zone, unit, and worker unit). A given covariate contributes significantly to the model fit when the 95% credible interval does not contain zero. PC=principal component.

creating breeding sites for the mosquito. Specifically, *A stephensi* breeds mainly in clean or clear water containers such as overhead water tanks, wells, cisterns, barrels or drums, sumps (underground tanks), roof gutters, curing pits in construction sites, fountains, and ornamental tanks.[56] The second component largely corresponds to variation in labour and employment, which is likely to relate to human mobility. Households relying on public and non-motorised transport typically correspond to poor socioeconomic status, including employment as casual labourers and low-skilled workers, and typically belong to socioculturally disadvantaged communities such as Scheduled Castes or Scheduled Tribes. Employment has also followed the outward growth in housing, thus creating commute patterns that are not only periphery to centre but also centre to periphery and periphery to periphery.[58,59] Movement of vectors is expected to act at very local scales because mosquitoes do not travel far[60] and typically stay within the same residence for days.[16] Finally, the third component is associated with population density, critical to epidemic spread, particularly in urban landscapes with pronounced heterogeneity in population distributions. Population density can influence individual risk of infection through its effect on the local abundance of mosquitoes.[61]

Here, population density (represented by PC3) increased malaria risk. For urban malaria, higher population density could result in higher water storage concentrations in close proximity to people. Our finding is consistent with that of Romeo-Aznar and colleagues,[61] who presented indirect evidence for an increase with human population density of the carrying capacity of vector abundance per human for dengue in poor areas of Delhi. The authors found that an increase faster than linear in poor areas of Delhi was sufficiently fast to generate a positive trend in the force of infection with human population. These findings differ from the typical assumptions in process-based temporal models for

coupled vector-human transmission, of either a constant population or a linear increase of vectors with human numbers. These assumptions imply a lower force of infection when the number of humans is higher, resulting in a lower malaria risk with higher population density. Thus, our finding further underscores that the effect of population density might not be properly parameterised in process-based models, depending on socioeconomic status, as suggested by Romeo-Aznar and colleagues.[61]

Despite limitations, our spatiotemporal statistical model captures the seasonal pattern and the main trends in interannual variation of malaria cases. The model can also predict the spatial variation in epidemic peaks for the period up to 2014 to a reasonable extent. Additionally, modelling malaria incidence rates at this resolution, rather than at coarser or finer scales, generates better predictions overall for each unit in the city, based on comparison of MAE between the best model and the baseline model. Goodness of fit measured with the pseudo-$R^2$ also shows that we can explain more spatiotemporal variability overall at this scale. Spatially explicit predictions decline in accuracy towards coarser levels, reflecting the averaging across heterogeneous effects, as seen in the reduced contribution of the structured random effect and the socioeconomic variables. At the finest scales, there is also a reduction in predictability, which could result from increased measurement noise in both malaria and covariates, and insufficient measurement resolution in covariates in general.

Future analysis will extend the data up to the present and improve on the sampling and calibration of covariates in space. There is clearly room for more detailed characterisation of microclimate and for explaining a larger fraction of the observed variability, including that captured so far by random effects. Resulting model improvements could help address whether the population dynamics of the disease exhibits a decreasing trend with intervention efforts when evaluated in the context of climate variability, and how such a trend varies in space. The model framework proposed here could be further improved by including mobility fluxes derived from movement models based on the spatial distribution of the population, to replace the near-neighbour effects in the spatial random effect. Temporal changes in city structure would also be informative, particularly the development of informal settlements and the local growth of the periphery with associated construction sites.

The current framework complements efforts to map and monitor in real time the spatiotemporal variability of urban malaria in India with Geographic Information Systems. For example, Srivastava and colleagues[62] describe such a system for a town in Tamil Nadu with a considerably smaller population than that considered here. Statistical modelling of cases in space and time provides a basis for an early-warning system informing control efforts. Given the time lags in the climate malaria transmission system, which typically span from 1 month to 3 months, observed climate variables incorporated in a model such as the one presented here can provide predictive lead capacity for forecasting malaria outbreaks ahead of the peak season. Random effects were incorporated in the formulation of the model to account for unaccounted factors in the covariates, including effects of control efforts, and for case reporting and surveillance error. Although the random effects account for substantial variability, consideration of the climate covariates reduced their size effect. Indication that the effects of specific covariates, including temperature and PC1, increase in significance at the finest spatial scale, suggests the value of better characterising spatial heterogeneity along these axes. Extension of the approach to other cities, including larger ones, and its sustained application over time, would provide a basis to evaluate similarities and differences, and to go from maps and alerts based solely on surveillance to predictions ahead of the season. Also, the larger number of potential environmental and socioeconomic covariates collected through such efforts could further inform summary variables such as the PCs used here.

Surat has experienced extensive malaria interventions in the past three decades, reflected in a negative trend in reported cases from the 1980s and 1990s to the 2000s. Since 2002, the city has had seasonal outbreaks of smaller size but nevertheless recurrent, with interannual variability but no monotonic trend in reported cases.[38] The stationary pattern of spatial risk described here, together with the major drivers of this variation, indicate that targeted control could help reduce transmission even further, and that control measures could be implemented ahead of the season based on known spatial heterogeneity. Ongoing efforts to provide better access to water might reduce the transmission of urban malaria and possibly that of other vector-borne infections. Although we could not separate the correlated effects of poverty and water access and storage here, this is an important area for further study. Ultimately, at longer time scales, a poverty reduction concomitant with better access to an uninterrupted water supply is fundamental to reducing and eliminating malaria within cities and at a regional and national level. A deeper understanding of the effects of relative humidity and temperature on urban malaria transmission, and their interplay with population growth, is essential to evaluating control in the context of climate variability and to building climate change scenarios for the disease. Both humidity and temperature are expected to increase under future climate projections for the Indian subcontinent,[3] specifically in the northwest of India.[2,57] A better understanding of how climate factors affect malaria transmission within urban environments could inform India's target of malaria elimination by 2030.

**Contributors**
MP and MS-V conceived and designed the study. MS-V and RL formulated the statistical model, and MS-V implemented the statistical analysis and wrote the first draft. MS-V, MP, RL, and LA analysed the data and the results from the models. KGV, VD, and AN provided expertise on the data and on the epidemiology of the region. All authors discussed the results and contributed to the final manuscript. The corresponding author had full access to all the data in the study and had final responsibility for the decision to submit for publication.

**Declaration of interests**
We declare no competing interests.

**Data sharing**
Code to fit the statistical model, and for other statistical analyses, as well as climate, demographic and socioeconomic data, have been deposited at the Github site (https://github.com/biomac-lab/Paper_lancet_Surat). An agreement with the Surat Municipal Corporation, the data provider, will be required for access to the epidemiological data.

**Acknowledgments**
We are grateful to the Surat Municipal Corporation commissioner for providing the malaria data for the city. We also thank Menno Bouma (independent scientist) for insightful discussions in the early stages of this project, and Vimal Mishra (Gandhinagar Institute of Technology, Gandhinagar, India) for technical advice on the calculation and interpolation of the humidity data, and on the analysis of the climate data. MP acknowledges the support of the National Institutes of Health ("Redefining thermal suitability for urban malaria transmission in the context of humidity", R01 AI153444–01, University of Chicago subaward to Cornell University, Courtney Murdock). RL was supported by a Royal Society Dorothy Hodgkin Fellowship and the IDExtremes project funded by the Wellcome Trust (226069/Z/22/Z). We thank the Gardner High Performance Computing cluster from the Center for Research Informatics of the University of Chicago for computational resources.

**References**

1 Harpham T. Urban health in developing countries: what do we know and where do we go? *Health Place* 2009; **15:** 107–16.
2 Vittal H, Ghosh S, Karmakar S, Pathak A, Murtugudde R. Lack of dependence of Indian summer monsoon rainfall extremes on temperature: an observational evidence. *Sci Rep* 2016; **6:** 31039.
3 Shepherd JM, Pierce H, Negri AJ. Rainfall modification by major urban areas: observations from spaceborne rain radar on the TRMM satellite. *J Appl Meteorol* 2002; **41:** 689–701.
4 Ahern M, Kovats RS, Wilkinson P, Few R, Matthies F. Global health impacts of floods: epidemiologic evidence. *Epidemiol Rev* 2005; **27:** 36–46.
5 Pickett STA, Cadenasso ML, Rosi-Marshall EJ, et al. Dynamic heterogeneity: a framework to promote ecological integration and hypothesis generation in urban systems. *Urban Ecosyst* 2017; **20:** 1–14.
6 Zhou W, Pickett STA, Cadenasso ML. Shifting concepts of urban spatial heterogeneity and their implications for sustainability. *Landsc Ecol* 2017; **32:** 15–30.
7 Bolay J-C. What sustainable development for the cities of the South? Urban issues for a third millennium. *Int J Urban Sustain Dev* 2012; **4:** 76–93.
8 Mishra V, Ganguly AR, Nijssen B, Lettenmaier DP. Changes in observed climate extremes in global urban areas. *Environ Res Lett* 2015; **10:** 024005.
9 Zhao L, Lee X, Smith RB, Oleson K. Strong contributions of local background climate to urban heat islands. *Nature* 2014; **511:** 216–19.
10 Alirol E, Getaz L, Stoll B, Chappuis F, Loutan L. Urbanisation and infectious diseases in a globalised world. *Lancet Infect Dis* 2011; **11:** 131–41.
11 Donnelly MJ, McCall PJ, Lengeler C, et al. Malaria and urbanization in sub-Saharan Africa. *Malar J* 2005; **4:** 12.
12 Hay SI, Guerra CA, Tatem AJ, Atkinson PM, Snow RW. Urbanization, malaria transmission and disease burden in Africa. *Nat Rev Microbiol* 2005; **3:** 81–90.
13 Qi Q, Guerra CA, Moyes CL, et al. The effects of urbanization on global *Plasmodium vivax* malaria transmission. *Malar J* 2012; **11:** 403.
14 De Silva PM, Marshall JM. Factors contributing to urban malaria transmission in sub-Saharan Africa: a systematic review. *J Trop Med* 2012; **2012:** 819563.
15 Cator LJ, Thomas S, Paaijmans KP, et al. Characterizing microclimate in urban malaria transmission settings: a case study from Chennai, India. *Malar J* 2013; **12:** 84.
16 Villena OC, Ryan SJ, Murdock CC, Johnson LR. Temperature impacts the environmental suitability for malaria transmission by *Anopheles gambiae* and *Anopheles stephensi*. *Ecology* 2022; **103:** e3685.
17 Santos-Vega M, Bouma MJ, Kohli V, Pascual M. Population density, climate variables and poverty synergistically structure spatial risk in urban malaria in India. *PLoS Negl Trop Dis* 2016; **10:** e0005155.
18 Wilson ML, Krogstad DJ, Arinaitwe E, et al. Urban malaria: understanding its epidemiology, ecology, and transmission across seven diverse ICEMR network sites. *Am J Trop Med Hyg* 2015; **93** (suppl)**:** 110–23.
19 Siraj AS, Bouma MJ, Santos-Vega M, et al. Temperature and population density determine reservoir regions of seasonal persistence in highland malaria. *Proc Biol Sci* 2015; **282:** 20151383.
20 Balkew M, Mumba P, Yohannes G, et al. An update on the distribution, bionomics, and insecticide susceptibility of *Anopheles stephensi* in Ethiopia, 2018-2020. *Malar J* 2021; **20:** 263.
21 Carter TE, Yared S, Gebresilassie A, et al. First detection of *Anopheles stephensi* Liston, 1901 (Diptera: culicidae) in Ethiopia using molecular and morphological approaches. *Acta Trop* 2018; **188:** 180–86.
22 Takken W, Lindsay S. Increased threat of urban malaria from *Anopheles stephensi* mosquitoes, Africa. *Emerg Infect Dis* 2019; **25:** 1431–33.
23 Faulde MK, Rueda LM, Khaireh BA. First record of the Asian malaria vector *Anopheles stephensi* and its possible role in the resurgence of malaria in Djibouti, Horn of Africa. *Acta Trop* 2014; **139:** 39–43.
24 Subbarao SK, Nanda N, Rahi M, Raghavendra K. Biology and bionomics of malaria vectors in India: existing information and what more needs to be known for strategizing elimination of malaria. *Malar J* 2019; **18:** 396.
25 Mnzava A, Monroe AC, Okumu F. *Anopheles stephensi* in Africa requires a more integrated response. *Malar J* 2022; **21:** 156.
26 Trusilova K, Früh B, Brienen S, et al. Implementation of an urban parameterization scheme into the regional climate model COSMO-CLM. *J Appl Meteorol Climatol* 2013; **52:** 2296–311.
27 Georgescu M, Morefield PE, Bierwagen BG, Weaver CP. Urban adaptation can roll back warming of emerging megapolitan regions. *Proc Natl Acad Sci USA* 2014; **111:** 2909–14.
28 Potter KA, Arthur Woods H, Pincebourde S. Microclimatic challenges in global change biology. *Glob Change Biol* 2013; **19:** 2932–39.
29 Murdock CC, Blanford S, Luckhart S, Thomas MB. Ambient temperature and dietary supplementation interact to shape mosquito vector competence for malaria. *J Insect Physiol* 2014; **67:** 37–44.
30 Thomas S, Ravishankaran S, Justin NAJA, et al. Resting and feeding preferences of *Anopheles stephensi* in an urban setting, perennial for malaria. *Malar J* 2017; **16:** 111.
31 Blanford S, Read AF, Thomas MB. Thermal behaviour of *Anopheles stephensi* in response to infection with malaria and fungal entomopathogens. *Malar J* 2009; **8:** 72.
32 Afrane YA, Klinkenberg E, Drechsel P, Owusu-Daaku K, Garms R, Kruppa T. Does irrigated urban agriculture influence the transmission of malaria in the city of Kumasi, Ghana? *Acta Trop* 2004; **89:** 125–34.
33 Pincebourde S, Murdock CC, Vickers M, Sears MW. Fine-scale microclimatic variation can shape the responses of organisms to global change in both natural and urban environments. *Integr Comp Biol* 2016; **56:** 45–61.
34 Evans MV, Bhatnagar S, Drake JM, Murdock CC, Mukherjee S. Socio-ecological dynamics in urban systems: an integrative approach to mosquito-borne disease in Bengaluru, India. *People Nat* 2022; **4:** 730–43.
35 Mathanga DP, Tembo AK, Mzilahowa T, et al. Patterns and determinants of malaria risk in urban and peri-urban areas of Blantyre, Malawi. *Malar J* 2016; **15:** 590.

36 Sharma VP. Re-emergence of malaria in India. *Indian J Med Res* 1996; **103:** 26–45.

37 Nagpal BN, Srivastava A, Dash AP. Resting behaviour of *Anopheles stephensi* type form to assess its amenability to control malaria through indoor residual spray. *J Vector Borne Dis* 2012; **49:** 175–80.

38 Santos-Vega M, Martinez PP, Vaishnav KG, et al. The neglected role of relative humidity in the interannual variability of urban malaria in Indian cities. *Nat Commun* 2022; **13:** 533.

39 Office of the Registrar General & Census Commissioner, India Ministry of Home Affairs, Government of India. Census tables. 2011. https://censusindia.gov.in/census.website/data/census-tables (accessed Aug 6, 2017).

40 Rathore A, Jasrai YT. Evaluating temperature and precipitation variability over Gujarat, India from 1957–2007. *Int J Sci Eng Res* 2013; **4:** 956–62.

41 Kevadiya S, Patel M, Modi J, Gamit B, Patel P, Padsala S. Characteristic and trends of malaria in Surat district of Gujarat: a hospital based study. *Int J Res Med Sci* 2014; **2:** 151.

42 Peng G, Li J, Chen Y, Norizan AP, Tay L. High-resolution surface relative humidity computation using MODIS image in Peninsular Malaysia. *Chin Geogr Sci* 2006; **16:** 260–64.

43 Anselin L. Spatial econometrics: methods and models. Dordrecht: Springer Dordrecht, 1988.

44 Anselin L. Local indicators of spatial association—LISA. *Geogr Anal* 2010; **27:** 93–115.

45 Fletcher IK, Stewart-Ibarra AM, Sippy R, et al. The relative role of climate variation and control interventions on malaria elimination efforts in El Oro, Ecuador: a modeling study. *Front Environ Sci* 2020; **8:** 135.

46 Grillet ME, Moreno JE, Hernández-Villena JV, et al. Malaria in southern Venezuela: the hottest hotspot in Latin America. *PLoS Negl Trop Dis* 2021; **15:** e0008211.

47 Fletcher IK, Grillet ME, Moreno JE, et al. Synergies between environmental degradation and climate variation on malaria re-emergence in southern Venezuela: a spatiotemporal modelling study. *Lancet Planet Health* 2022; **6:** e739–48.

48 Colón-González FJ, Soares Bastos L, Hofmann B, et al. Probabilistic seasonal dengue forecasting in Vietnam: a modelling study using superensembles. *PLoS Med* 2021; **18:** e1003542.

49 Rue H, Martino S, Chopin N. Approximate Bayesian inference for latent Gaussian models by using integrated nested Laplace approximations. *J R Stat Soc Series B Stat Methodol* 2009; **71:** 319–92.

50 Besag J, York J, Mollié A. Bayesian image restoration, with two applications in spatial statistics. *Ann Inst Stat Math* 1991; **43:** 1–20.

51 Lowe R, Cazelles B, Paul R, Rodó X. Quantifying the added value of climate information in a spatio-temporal dengue model. *Stochastic Environ Res Risk Assess* 2016; **30:** 2067–78.

52 Mordecai EA, Paaijmans KP, Johnson LR, et al. Optimal temperature for malaria transmission is dramatically lower than previously predicted. *Ecol Lett* 2013; **16:** 22–30.

53 Parham PE, Michael E. Modeling the effects of weather and climate change on malaria transmission. *Environ Health Perspect* 2010; **118:** 620–26.

54 Perkins TA, Scott TW, Le Menach A, Smith DL. Heterogeneity, mixing, and the spatial scales of mosquito-borne pathogen transmission. *PLOS Comput Biol* 2013; **9:** e1003327.

55 Reiner RC Jr, Smith DL, Gething PW. Climate change, urbanization and disease: summer in the city…. *Trans R Soc Trop Med Hyg* 2015; **109:** 171–72.

56 Thomas S, Ravishankaran S, Justin JA, et al. Overhead tank is the potential breeding habitat of *Anopheles stephensi* in an urban transmission setting of Chennai, India. *Malar J* 2016; **15:** 274.

57 Dai A. Precipitation characteristics in eighteen coupled climate models. *J Clim* 2006; **19:** 4605–30.

58 Shirgaokar M. Employment centers and travel behavior: exploring the work commute of Mumbai's rapidly motorizing middle class. *J Transp Geogr* 2014; **41:** 249–58.

59 Srinivasan KK, Bhargavi PVL, Ramadurai G, Muthuram V, Srinivasan S. Determinants of changes in mobility and travel patterns in developing countries: case study of Chennai, India. *Transp Res Rec* 2007; **2038:** 42–52.

60 Quraishi MS, Mofidi MH, Motabar M, et al. Determination of flight range and length of gonotrophic cycles in nature in *Anopheles stephensi* with the aid of P32. 1965. https://iris.who.int/handle/10665/65282 (accessed Sept 12, 2017).

61 Romeo-Aznar V, Paul R, Telle O, Pascual M. Mosquito-borne transmission in urban landscapes: the missing link between vector abundance and human density. *Proc Biol Sci* 2018; **285:** 20180826.

62 Srivastava A, Nagpal BN, Saxena R, et al. GIS based malaria information management system for urban malaria scheme in India. *Comput Methods Programs Biomed* 2003; **71:** 63–75.